

Exploring the effects of biophysical parameters on the spatial pattern of rare cold damage to mangrove forests



Kai Liu^a, Lin Liu^{a,b,*}, Hongxing Liu^b, Xia Li^a, Shugong Wang^a

^a School of Geography and Planning, Center of Integrated Geographic Information Analysis, Sun Yat-sen University, Guangzhou 510275, China

^b Department of Geography, University of Cincinnati, Cincinnati 45221, USA

ARTICLE INFO

Article history:

Received 28 March 2011

Received in revised form 7 April 2014

Accepted 10 April 2014

Available online xxxx

Keywords:

Mangroves

Cold damage

IKONOS

Object-oriented classification

Climate and landscape controls

Biophysical parameters

ABSTRACT

In recognition of the role of mangrove forests as natural barriers and bio-shields in protecting coastal population and property in the aftermath of the 2004 Indian Ocean tsunami disaster, many Asian countries have launched various projects to restore and conserve mangrove trees. The growth and vitality condition of mangroves may be negatively influenced by various anthropogenic and natural disturbances and stresses, such as cold weather events. This paper represents the first attempt to map the cold damage to mangroves in the tropical zone of Southern China using high resolution multispectral satellite imagery. In this study, the spatial distribution of severity level of cold damage to mangroves imposed by a rare blizzard in Southern China during early 2008 has been mapped and analyzed using IKONOS image. An object-oriented classification applied to the images achieved an overall accuracy of 90.9% for classifying mangroves into three categories: undamaged, damaged, and dead. Of the total 287.30 ha of mapped mangroves, approximately 51.1% were damaged or died due to the cold stress of the blizzard. These results have been verified by more recent WorldView-II images. Furthermore, we explored the associations between the cold damage severity level of mangroves and climate and landscape factors, including elevation, surface slope, aspect, wind direction and velocity, wind shadow effect, and tree height. The surface topographical variables are derived from the ASTER Global DEM. The analysis results suggest that wind direction, terrain topography, and proximity to ocean are important local environmental factors controlling the vulnerability of mangroves to cold damage. Most damaged mangroves were located near the open sea, as a result of a possible edge exposure effect. The damage to the mangroves on the leeward side of a hill was also minimal. Such knowledge of climate and landscape controls can offer insight on how to better restore and protect the mangrove forest in the future.

© 2014 Elsevier Inc. All rights reserved.

1. Introduction

Mangrove forests consist of salt-tolerant tree species that grow in the intertidal zone of tropical and subtropical coasts, particularly in sheltered bays, lagoons, and estuaries (Blasco et al., 1998; Everitt & Judd, 1989; Heumann, 2011; Wang et al., 2003). Mangroves are one of the most productive ecosystems in the world and provide a variety of ecological and societal goods and services. Mangrove vegetation itself has been harvested directly as food supplements and timber products (Green, Clark, Mumby, Edwards, & Ellis, 1998; Kuenzer, Bluemel, Gebhardt, Quoc, & Dech, 2011). In addition, mangrove forests have been also utilized by human beings for fishing, recreation, and aquaculture. Their functions in absorbing pollution, purifying ocean water, and maintaining coastal biodiversity have been widely recognized (Blasco,

Saenger, & Janodet, 1996; Heumann, 2011; Murray et al., 2003; Sheridan & Hays, 2003). Inhabiting the interface between land and sea at low latitudes, mangroves are adapted to many harsh environmental conditions, such as being subjected to daily tidal changes in temperature, water and salt exposure, and varying degrees of anoxia (Alongi, 2008). Meanwhile, mangrove forests are among the most threatened global ecosystems (Ellison & Farnsworth, 1996). Valiela, Bowen, and York (2001) reported that a considerable portion of global mangrove area has lost in the past two decades. Giri et al. (2008) estimated that 12% of tropical mangrove forests in the tsunami-impacted regions of Indonesia, Malaysia, Thailand, Myanmar, Bangladesh, India, and Sri Lanka have been destroyed during 1975–2005 due to agriculture encroachment, aquaculture/shrimp farming, and urban development.

Following the devastating aftermath of the 2004 Indian Ocean tsunami in Southeast Asia, there is growing empirical and field observational evidence that mangroves are particularly valuable in protecting coastal population, settlements, and infrastructure from tsunami attacks by reducing wave amplitude and energy (Alongi, 2008; Dahdouh-Guebas et al., 2005; Danielsen et al., 2005; Kathiresan & Rajendran, 2005; Sanford, 2009; Tanaka, Sasaki, Mowjood, Jinadasa,

* Corresponding author at: Department of Geography, University of Cincinnati, Cincinnati, USA.

E-mail addresses: liuk6@mail.sysu.edu.cn (K. Liu), liulin2@mail.sysu.edu.cn (L. Liu), Hongxing.Liu@uc.edu (H. Liu), lixia@mail.sysu.edu.cn (X. Li), esswsg@mail.sysu.edu.cn (S. Wang).

& Homchuen, 2007). In recognition of the critical role of mangroves as natural barriers and bio-shields against tropical storms and tsunamis, many countries such as Indonesia, Thailand, and Sri Lanka have launched various projects to replant and restore the degraded and deforested mangrove areas in order to enhance the overall resilience of coastal areas to natural hazards (Barbier, 2006; Harakunarak & Aksornkoae, 2005). A great effort has been made in China to conserve and restore mangroves, particularly in Guangdong and Hainan provinces where fast-growing mangrove species have been introduced to their deforested mangrove wetlands (Li et al., 1998; Ren et al., 2008, 2011; Xiao, Chen, & Xie, 2004).

Mangrove ecosystems are subject to a variety of natural and anthropogenic disturbances, which may vary in their duration, frequency, size, and intensity. Several researches have monitored the change or explored spatial pattern of mangrove forests affected by these disturbances, such as forest fire (Dahdouh-Guebas, Van Pottelbergh, Kairo, Cannicci, & Koedam, 2004), hurricane (Ross et al., 2006), aquaculture farming (Thu & Populus, 2007), and urban sprawl (Zhang et al., 2008), etc. Mangrove tree species are fairly robust and highly tolerant to water-logged saline soils in subtropical and tropical environments, but are extremely vulnerable to cold temperatures (Stevens, Fox, & Montague, 2006; Stuart, Choat, Martin, Holbrook, & Ball, 2007). In subtropical areas, particularly in areas near the latitudinal limit of mangrove distribution, frosts and freezes associated with severe cold weather events may act as disturbances that devalue, damage, or kill mangrove trees. For example, mangroves in southern Florida, Texas, and Louisiana have been periodically damaged or killed by freezes (Everitt, Yang, Sriharan, & Judd, 2008; Ross et al., 2006; Ross, Ruiz, Sah, & Hanan, 2009; Stevens et al., 2006; Stuart et al., 2007). In Florida, average winter minimum temperature ranges from 8.2 to 9.5 °C, but cold temperatures as severe as −10 °C are regular events, occurring once every 8 years over the past century on average (Ross et al., 2009; Stevens et al., 2006; Stuart et al., 2007). In southern Australia, mangroves were often injured by mild frosts at least once a year (Stuart et al., 2007). In subtropical China, freezing temperatures sporadically occur, causing substantial frost damage to mangroves (Li, Liao, Guan, Zheng, & Chen, 2009; Xiao et al., 2004). In early 2008, a blizzard swept the coast of Southern China. It severely damaged a total of 7930 km² of forests, including mangroves, in Guangdong Province (Chen, Wang, Zhang, Huang, & Zhao, 2010; Li et al., 2009).

With increasing concern on extremely climate events, many studies have focused on damaged mangrove forests affected by cold events (Chen et al., 2010; Jiang & Huang, 2008; Ross et al., 2009). The landscape structure and community composition of mangrove forests influenced by cold events have been explored in these studies. However, current studies about cold damages to mangrove forests mainly focused on native mangrove forests. To date, the importance of introduced and replanted mangrove forests has not been given sufficient attention. These mangrove forests are more sensitive to the decline of temperature. To mitigate and prevent the cold damage to the replanted mangroves in tropical and subtropical areas, an effective technique for detecting and mapping the mangrove damage due to cold weather is much needed. Such technique can also help develop an understanding of local environmental factors controlling the vulnerability of the mangroves to the cold damage.

In recent decades, remote sensing techniques have been widely applied in mangrove studies. Selective applications include mapping the spatial extent of mangrove distribution (Gao, 1998; Green et al., 1998; Held, Ticehurst, Lymburner, & Williams, 2003; Vaiphasa, Skidmore, & de Boer, 2006), monitoring mangrove dynamic changes (Conchedda, Durieux, & Mayaux, 2008; Kovacs, Wang, & Blanco-Correa, 2001; Liu, Li, Shi, & Wang, 2008; Sulong, Mohd-Lokman, Mohd-Tarmizi, & Ismail, 2002; Vijay et al., 2005), estimating mangrove leaf area index (LAI) (Kovacs, Flores-Verdugo, Wang, & Aspden, 2004), and calculating mangrove biomass (Laliberte, Fredrickson, & Rango, 2007). Remotely sensed data used in previous mangrove studies include aerial

photographs (Fromard, Vega, & Proisy, 2004; Sulong et al., 2002), SPOT XS (Franklin, 1993; Gao, 1998; Pasqualini et al., 1999), Landsat TM/ETM+ (Conchedda et al., 2008; Liu et al., 2008; Long & Skewes, 1996), SAR (Baghdadi & Oliveros, 2007; Kovacs, Vandenberg, Wang, & Flores-Verdugo, 2008; Pasqualini et al., 1999), ASTER (Vaiphasa et al., 2006), and IKONOS and QuickBird data (Everitt et al., 2008; Laba et al., 2010; Wang, Sousa, Gong, & Biging, 2004). In addition, LiDAR remote sensing has been used in recent years to study the morphology, biomass and dynamics of the mangrove forests (Zhang et al., 2008).

However, no research effort has been reported in using remote sensing technique to detect and map the cold damage to mangrove forests, especially in tropical areas. Until now, it is unknown if multispectral satellite image data contain sufficient information to assess the mangrove damage due to cold weather. In addition, the relationship between environmental factors and pattern of damaged mangrove forests affected by cold events at a landscape-scale has not gained sufficient attention, especially for replanted or restored fast-growing mangrove forests. To fill this research gap, we intend to explore the applicability of the high resolution multispectral satellite images and object-oriented classification method for detecting and mapping the severity level of mangrove cold damage by the 2008 blizzard on Qi'ao Island of Guangdong Province. Post-blizzard IKONOS multispectral (4 m) and panchromatic (1 m) images are used in the study. Furthermore, this paper examines possible associations between local environmental factors and the severity of mangrove damage using a correspondence analysis method. Environmental factors under investigation include climate variables and biotic/abiotic landscape factors, which were derived from ASTER Global Digital Elevation Model (GDEM). A better understanding of local climate and landscape controls on mangrove could offer useful insights on how to better conserve, protect and manage mangrove forests in the future.

2. Study area and data preparation

2.1. Study area

Qi'ao Island, with an area of about 24 km², is located in the west of the Pearl River Delta, near the City of Zhuhai in Southern China (Fig. 1). The island spans between latitude 22°23'40"N–22°27'38"N, and enjoys warm tropical and subtropical climate with abundant rainfall. Its average annual precipitation ranges from 1700 mm to 2200 mm, and average annual temperature is between 22 °C and 23 °C. January is the coldest month, and the average temperature in this month is 15.3 °C. The climate is very suitable for the growth of mangroves, and the island has been designated a Mangrove Nature Reserve in Guangdong province, China. Previous studies (Jiang & Huang, 2008; Li et al., 2009) indicate that the daily average temperature higher than 10 °C in the coldest month is required for growing of mangrove forest in South China. Otherwise, mangrove trees will stop growing and parts of mangroves will be damaged. If frosty or extremely cold weather (temperature lower than 5 °C) lasts more than 2 days, mangrove forests will be damaged (Li et al., 1998). The damaged mangrove inside the Mangrove Nature Reserve on Qi'ao Island by the unusually cold weather during the 2008 blizzard is the focus of this research.

The Mangrove Nature Reserve is the largest wetland restoration project in China. Five mangrove species, including *Kandelia candel*, *Acanthus ilicifolius*, *Aegiceras corniculatum*, *Sonneratia caseolaris*, and *Sonneratia apetala*, were planted on the island. *K. candel* and *A. corniculatum* are located in the upper intertidal near the embankment in the study area. The other three mangrove species are planted in the mid-intertidal and lower intertidal, showing zonal distribution. The mangrove species also differ in tree height. *S. caseolaris* and *S. apetala* are the tallest mangrove species in the Qi'ao Island, which height ranging from 4 m to 12 m. *A. ilicifolius*, *A. corniculatum*, and *K. candel* average 1.5–2 m, 2.5–3.0 m, and 3–4 m in height, respectively. There also exists a

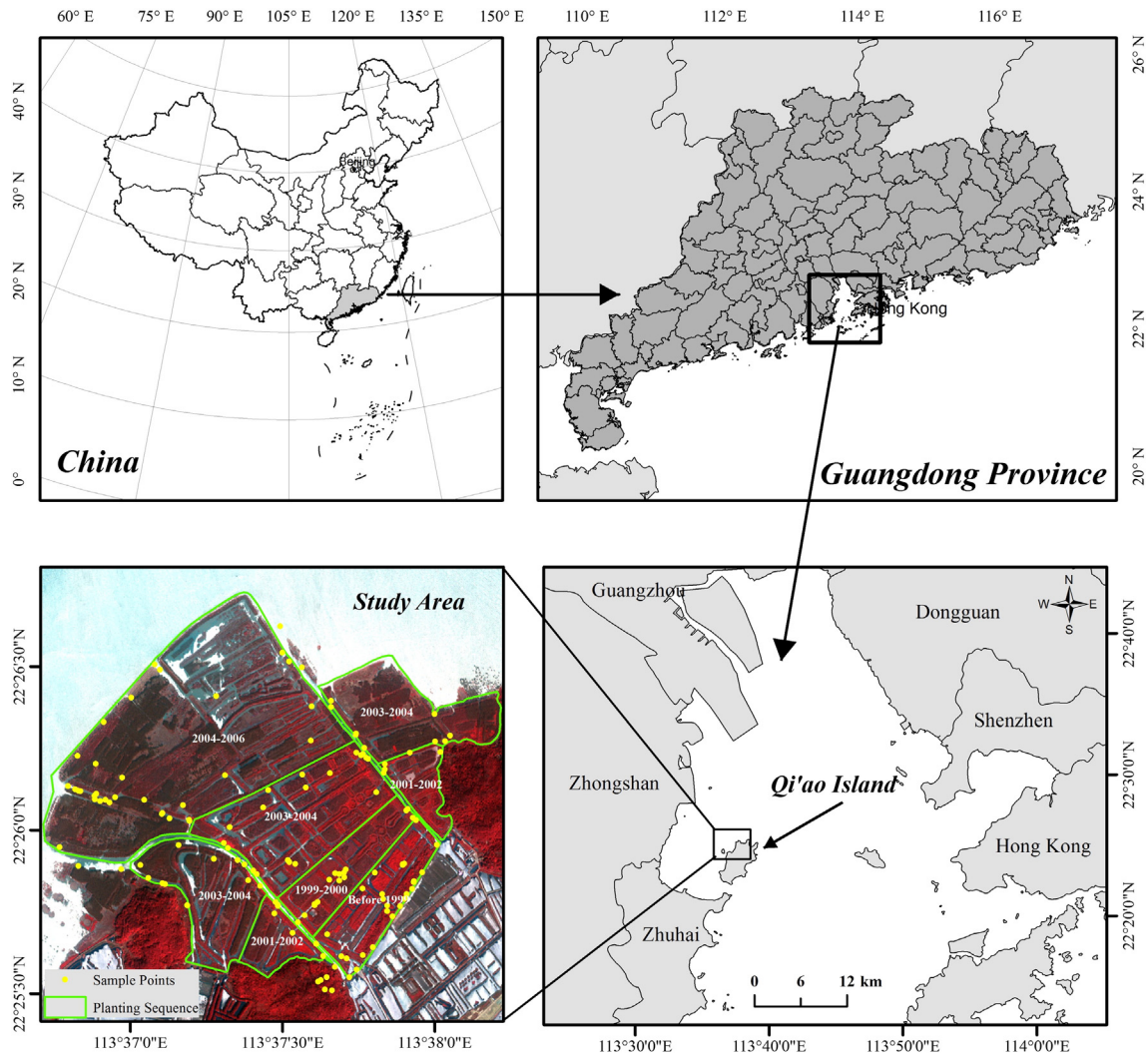


Fig. 1. Location of Qi'ao Island.

mangrove nursery stand at the seaward fringe in the east part of the study area. Most of young mangrove forests are *S. caseolaris* and *S. apetala* with a height lower than 1.5 m. Compared with the two introduced mangrove species in *S. caseolaris* and *S. apetala*, the native mangrove species *K. candel*, *Acanthus ilicifolius*, and *A. corniculatum* are more adaptive to local climate and less susceptible to extremely cold weather (Laliberte et al., 2007; Li et al., 2009).

2.2. Data preparation

The remotely sensed data used in this research is high-resolution IKONOS satellite image. It contains four multispectral bands (blue, green, red, and near-infrared) with a 4-m resolution and a panchromatic band with 1-m resolution. The image (about 4000×2500 pixels), acquired from GeoEye, Inc., was captured on 27 February, 2008, two weeks after the blizzard. The image is radiometrically and geometrically corrected, and projected to the UTM zone 49 N coordinate system. A subset of the image covering the Mangrove Nature Reserve is used in this research (Fig. 1).

The ancillary data used in this research include ASTER GDEM and climate records. The ASTER GDEM is developed jointly by the U.S. National Aeronautics and Space Administration (NASA) and Ministry of Economy, Trade, and Industry (METI) of Japan, and covers land surfaces between 83°N and 83°S (Hayakawa, Oguchi, & Lin, 2008). The ASTER GDEM has a spatial resolution of 1 arc-second (30 m) and is referenced

to the WGS84/EGM96 geoid. A subset of the ASTER GDEM is extracted for our case study area, and resampled into a 4-m elevation grid to match the resolution of IKONOS multispectral images by using a bilinear resampling method. The climate data, including wind speed, wind direction and temperature, are obtained from Zhuhai Bureau of Meteorology. The daily mean temperature between January and February 2008 is summarized in Fig. 2. The daily mean temperature from 23 January to 14 February is consistently below 10°C , which is 6.5°C below normal. From 31 January to 2 February, the daily mean temperature is below 5°C , which causes most severe damage to the mangrove forest. The dominant wind in this period blows from the East (Fig. 3). Although the lowest temperature in Qi'ao Island during this period is below 0°C , a few ice crystals were found by the sea near Qi'ao Island and some regions to the immediate north of this island suffered frozen rain and snow disasters during these two months.

Two field observations were carried out on March 15–16, 2008 and November 19, 2008, to survey the damage level of mangrove forests. Given the constraint on accessibility via boat, a total of 35 sampling sites were selected to represent the study area. For each sampling site, a GPS was used to record the precise location, and mangrove cold damage severity level was observed within a $10 \times 10 \text{ m}^2$ plot of each site. The locations of 220 removed dead mangrove plots were identified on the image and confirmed by those who actually participated in the removal, and these locations were later verified on more recent WorldView-II images.

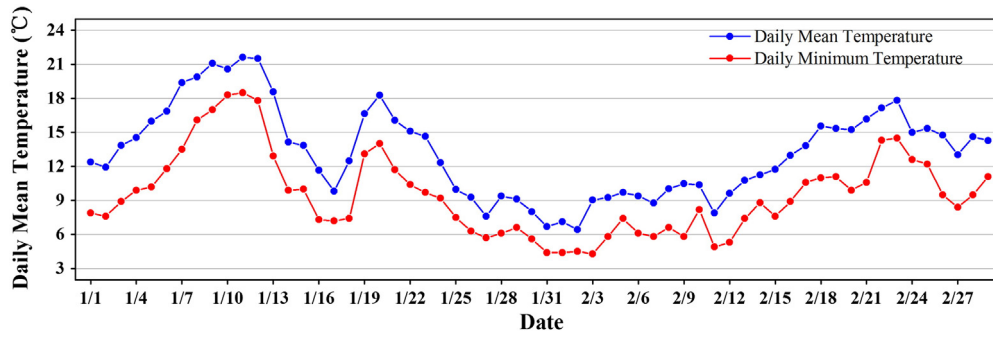


Fig. 2. Daily mean temperatures between 1 January and 28 February 2008.

3. Methodology

3.1. Damaged mangrove detection based on object-oriented classification method

First, damaged mangroves are detected using high spatial resolution remotely sensed data. The detection is based on an object-oriented classification method, which operates on image objects that are extracted through image segmentation, rather than on individual pixels (Duro, Franklin, & Dubé, 2012; Mitri & Gitas, 2004).

3.1.1. Spectral signature analysis of cold damage to mangroves

Three types of mangrove trees are observed after the blizzard period: undamaged, damaged, and dead. Dead mangroves are those with broken trunk or already died, damaged mangroves are those with the loss of foliage or broken branches, and undamaged mangroves refer to those surviving the blizzard without the significant defoliation. To detect these three levels of damages due to cold weather in IKONOS multispectral images, we need to understand the spectral responses of the undamaged, damaged and dead mangroves in different wavelength intervals. Training data are selected respectively for undamaged, damaged, and dead mangroves based on field observations. The mean DN value for each spectral band is used to characterize the spectral property of mangroves with different cold damage severity levels. As shown in Fig. 4a, the undamaged mangroves have stronger reflectance

than the damaged mangroves in all four spectral bands, particularly in the near infrared band. The dead mangroves have stronger reflectance in visible bands (blue, green, and red), but considerably lower reflectance in the near infrared (NIR) band than undamaged mangroves. The spectral curves of the mangroves of three damage severity levels in Fig. 4a also show a strong contrast in the spectral slope between red band and NIR band. To reduce the environmentally induced variations in the DN values of a single band and to take advantage of spectral slopes, the Normalized Difference Vegetation Index (NDVI) is calculated for these three types of mangroves. NDVI significantly enhances variations in the slopes of the spectral reflectance curves between red and near infrared bands that may otherwise be masked by the pixel brightness variations in each of the bands. As shown in Fig. 4b, the undamaged mangroves have a high positive NDVI value due to its strong reflectance in NIR band and absorption in the visible red band. The dead mangroves, without green leaf vegetation biomass, yield a negative NDVI value due to a larger reflectance in the red band than in the NIR band. The NDVI value for damaged mangroves is positive but small due to their similar reflectance in both red and NIR bands. It is evident that NDVI significantly enhances the discrimination of damaged and dead mangroves from undamaged ones.

3.1.2. Object-oriented classification

Traditional per-pixel classification method solely relies on the spectral information of a single pixel, often resulting in noisy clutter classification pattern (known as salt-and-pepper effect). The object-oriented image classification method represents a different paradigm for image analysis and understanding. This method first segments an image into a set of homogenous objects, and then classifies those objects into different categories. The basic spatial units in object-oriented image classification are image objects rather than individual image pixels. In addition to the spectral information, the object-oriented image classification method is capable of utilizing semantic information (e.g., size, shape, texture and contextual) of image objects and the spatial relationships (e.g., topological relationship) between them, which are ignored in the traditional per-pixel method. Previous studies have demonstrated that the object-oriented classification method can avoid some drawbacks of the traditional per-pixel classification and can often result in a higher classification accuracy.

3.1.2.1. Image segmentation. Image segmentation is the first step in object-oriented analysis, and meaningful image objects can be extracted in this process (Raši et al., 2011; Scepan, 2002). The image segmentation in this research has been carried out using Definiens 7.0 (also known as eCognition) software. The segmentation technique in Definiens is a bottom-up region merging technique where smaller image objects are merged into larger ones with the scale parameter controlling the growth in heterogeneity between adjacent image objects. The region merging function stops when image object growth exceeds the threshold defined by the scale parameter – the maximum allowable

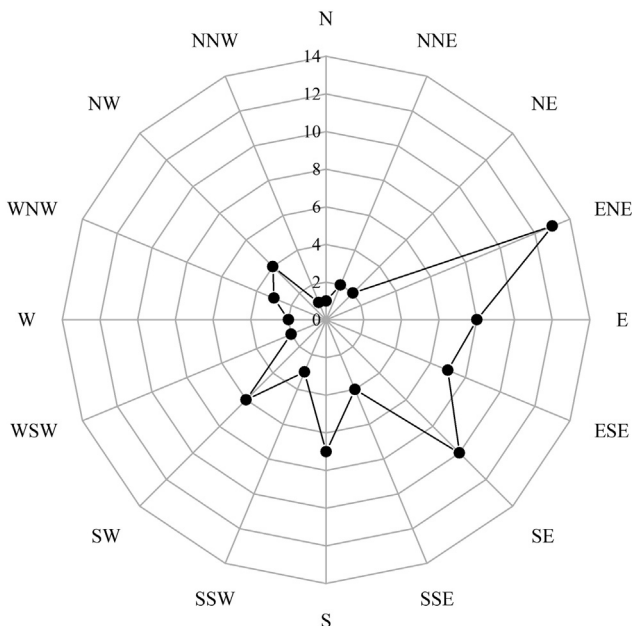


Fig. 3. Wind rose diagram for wind direction during the blizzard.

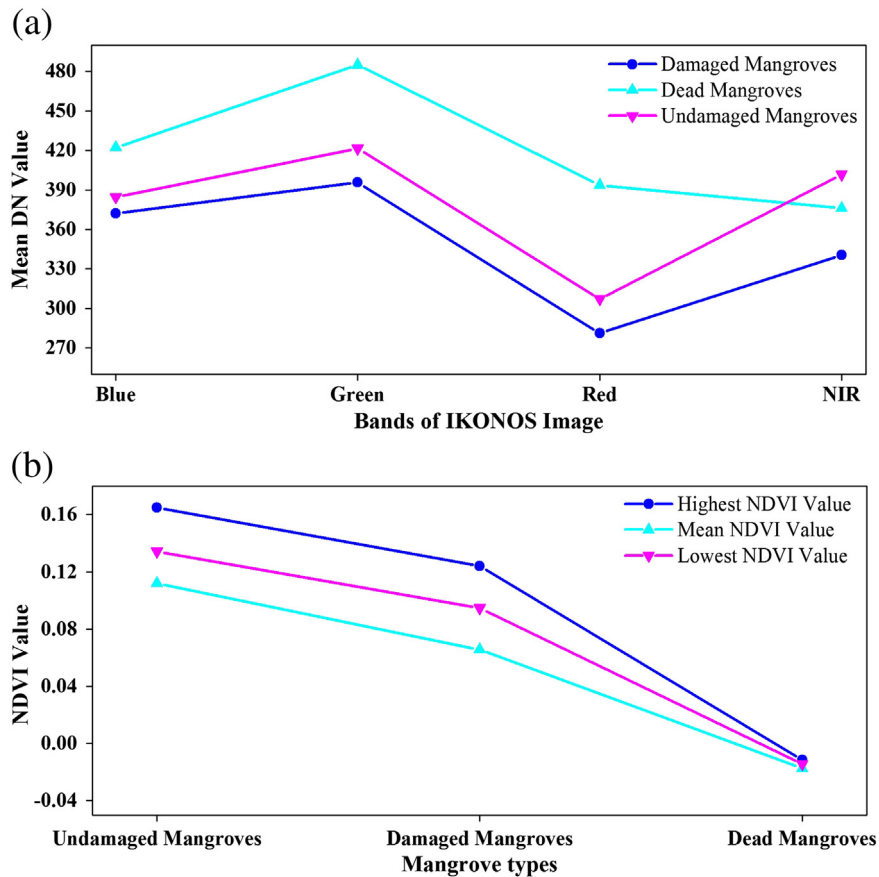


Fig. 4. Spectral and NDVI characteristics of cold damage to mangroves: a) spectral characteristics of cold damage to mangroves, b) NDVI characteristics of cold damage to mangroves.

heterogeneity of image object (Benz, Hofmann, Willhauck, Lingenfelder, & Heynen, 2004; Laliberte et al., 2007). Adjusting the scale parameter influences the average object size (Baatz & Schape, 2000). A small value of scale parameter results in a smaller average size of image objects. The color parameter, ranging from 0 to 1, determines the weight of spectral (color) heterogeneity against shape heterogeneity in the total image object heterogeneity. Previous studies suggest that more meaningful objects are extracted with a higher weight for the color criterion (Dronova, Gong, & Wang, 2011; Laliberte et al., 2004, 2007; Mathieu, Aryal, & Chong, 2007). The shape heterogeneity is further defined as a weighted sum of smoothness (the ratio of the border length and the shortest possible border length of the bounding box of an image object) and compactness (the ratio of the border length and the square root of the number of object pixels). The compactness parameter (0–1) gives the weight of the compactness versus the smoothness in the shape heterogeneity (Walker & Briggs, 2007). A recursive process of segmentation using different scale parameters results in a sequence of nested image objects with a different average size, which can construct a multi-level network of image objects. This network provides the basis for further information extraction and classification (Benz et al., 2004; Raši et al., 2011).

Table 1
Parameter of multi-scale segmentation.

Segmentation level	Scale	Color	Shape	Compactness	Smoothness
First level	200	0.8	0.2	0.4	0.6
Second level	30	0.7	0.3	0.4	0.6
Third level	10	0.7	0.3	0.4	0.6

3.1.2.2. *Damaged mangroves classification with decision tree method.* In this study, based on a series of tests by using an iterative “trial-and-error” approach, we determined appropriate parameters and obtained the three levels of segmentations. Equal weight is given to each spectral band for defining the spectral (color) heterogeneity. Table 1 shows the scale, color, shape and compactness parameter values used in our multi-scale segmentation process.

A two-stage classification method is performed based on the three scales of segmentations. As shown in Fig. 5, in the first stage the land cover on Qi’ao Island is classified into four general categories: Mangrove distributed area, sea, other forests, and other land-cover. The first stage of classification is based on the first level of segmentations. With the scale parameter of 200, the IKONOS image is segmented into relatively large image objects. A number of typical image objects are visually selected for each land cover type as training samples. Based on the training samples, a threshold value for each land cover type is determined in terms of red and infrared bands, and NDVI. All image objects are then classified into the four general land covers using these threshold values as the classifier.

In the second stage, the mangrove distributed areas obtained in the first stage are further classified into six sub-classes: undamaged mangroves, damaged mangroves, dead mangroves, other vegetation, mud, and tidal creek. The image objects classified as the mangrove distributed area in the first stage are further segmented into smaller image objects with a scale parameter of 30. Then, decision tree learning method implemented in the data mining software tool See5 (Quinlan, 1990, 1999) is applied to classify these small image objects into the six sub-classes.

The decision tree method is one of the most effective inductive machine learning techniques. Compared with traditional classification methods such as the maximum likelihood classifier and the linear

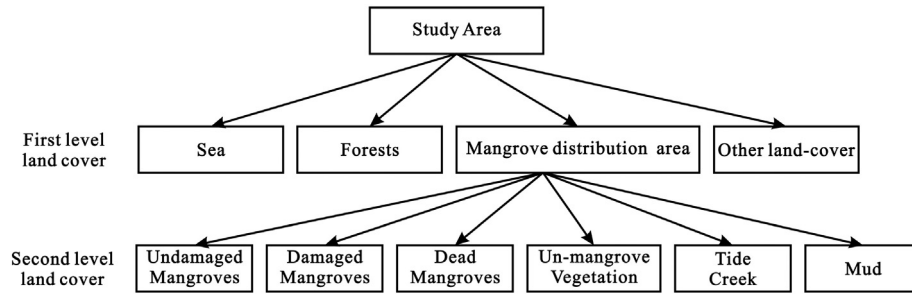


Fig. 5. Two-stage land cover type classification based on multi-scale segmentations.

discriminant function classifier, the decision-tree method has a number of advantages (DeFries & Chan, 2000; Hansen, Dubayah, & Defries, 1996). As a nonparametric classifier, it makes no assumptions regarding the statistical distribution and its parameters for input attribute data. It is also robust with respect to nonlinear and noisy relations among input attributes and class labels. The attributes for image objects generally do not follow the normal distribution, and certain level of linear or nonlinear relations exists among these attributes and between attributes and class labels. Therefore, for the image object classification, the decision-tree method is a better choice than the commonly used maximum-likelihood classification method, which assumes the normal distribution of input attribute for each class.

The decision-tree method involves several classification steps: preparing training data, selecting informative attributes, creating a decision tree, generating decision rules, assigning class labels to image objects, and evaluating classification accuracy. As an inductive machine learning technique, the decision tree method requires only a small set of good examples to function as training data (Quinlan, 1999). A total of 135 image objects, 30 objects for each of mangrove types and 45 objects for other three non-mangrove types, were surveyed in the field to serve as training data for generating the classification rule set.

Attributes of each object, used in this study, were derived from the five original bands of IKONOS image, including four multi-spectral bands and one panchromatic band. We generated 24 features for each object. These attributes were considered as initial input variables to train and construct the decision tree:

- 10 spectral attributes: Mean values and standard deviation values of blue, green, red, NIR, and panchromatic bands for each image object;
- 8 texture attributes: GLCM (Gray Level Co-occurrence Matrix) based indicators and GLDV (Gray Level Difference Vector). GLCM is a tabulation of how often different combinations of gray levels of two pixels at a fixed relative position occur in an image (Laliberte et al., 2007; Yu et al., 2006). The texture indicators generated from GLCM include homogeneity, contrast, dissimilarity, entropy, standard deviation and correlation. GLDV is the sum of the diagonals of the GLCM. GLDV entropy and GLDV contrast are calculated as well.
- 5 geometric and shape attributes: area, length/width, shape index, roundness and width of each image object;
- 1 vegetation attribute: NDVI value for each image object.

These attributes are considered as the initial candidate input variables, but not all the above attributes are actually used to construct the decision-tree for the cold damaged mangrove classification. The software tool See5 has a built-in winnowing function (Quinlan, 1999) for optimally selecting most useful attributes that have a relatively high discrimination capability. By using the winnowing function of See5 software, we analyze the training dataset and select the following attributes from the above list for generating classification rules: NDVI, standard deviation values of green, mean red, mean NIR. The decision tree is constructed in two steps. First, a large tree is grown to fit the training data closely. Then, the tree is pruned by removing parts that are predicted to have a relatively high error rate. This pruning process

corrects the over-fitting problem and reduces the size of the overall tree, resulting in reliable and compact decision rules (Quinlan, 1996). A pruning rate, a parameter used to address the trade-off between classification accuracy and decision tree size, is set to 25%. In order to obtain a steady training accuracy, a 10-fold cross-validation method is selected to analyze the training dataset because 10-fold cross-validation can use all training data for both of training and validation. The binary decision tree is then translated into a set of simple if-then rules. By applying if-then rules, the image objects of the mangrove distributed area are classified into the six sub-classes. The multi-scale segmentations and classification process for extracting the cold damaged mangrove forests are shown in Fig. 6. A total of 18 classification rules with a satisfied training accuracy of 89.3% are generated by using samples for decision tree classification. For post-classification error checking and correction, the classified image objects are further segmented into smaller units – the lowest scale of image objects with a scale parameter of 10. All these image objects are visually inspected, and mis-classified objects are manually corrected at this lowest scale. A final classification map is created.

3.1.2.3. Accuracy assessment of image classification. Based on a field survey sample, a contingency error matrix is created to assess the accuracy of the classification result from the decision tree learning method. A stratified random sampling approach was adopted to select the sample objects from the sample map drew during the second stage of field investigation (Congalton, 1988; Congalton & Mead, 1986; Nishii & Tanaka, 1999). A total of 177 sample objects were selected and used for accuracy assessment from all of 220 objects in the sample map. The selected sample objects mirror the overall distribution of different land cover categories. The accuracy assessments are carried out using Definiens 7.0 software, based on the error matrix from the field reference data.

3.2. Factors analysis on the vulnerability of mangroves to cold damage

Furthermore, the assumption that local environmental factors may change climate conditions and hence affect the severity level of cold damage to mangroves is consistent with spatial pattern of the mangrove cold damage index (MCDI) and correspondence analysis result as well as our field survey results.

3.2.1. Environmental factor definition and analysis

Environmental factors under investigation include climate variables (air temperature, wind direction and velocity) and local landscape variables (elevation, surface slope, and tree height). Mangrove forests are located in an open and flat area in the northwest of Qi'ao Island. The cold damage to mangroves during the blizzard could be caused by cold wind/air. In this paper, the leeward side distance to the hill ridges (Fig. 7b) is used as a proxy variable for the combined effect of wind direction and local landscape on the air temperature and wind velocity. The distance to the ocean water (Fig. 7a) is also used as a proxy variable for the possible edge effect near the coastline. This distance variable

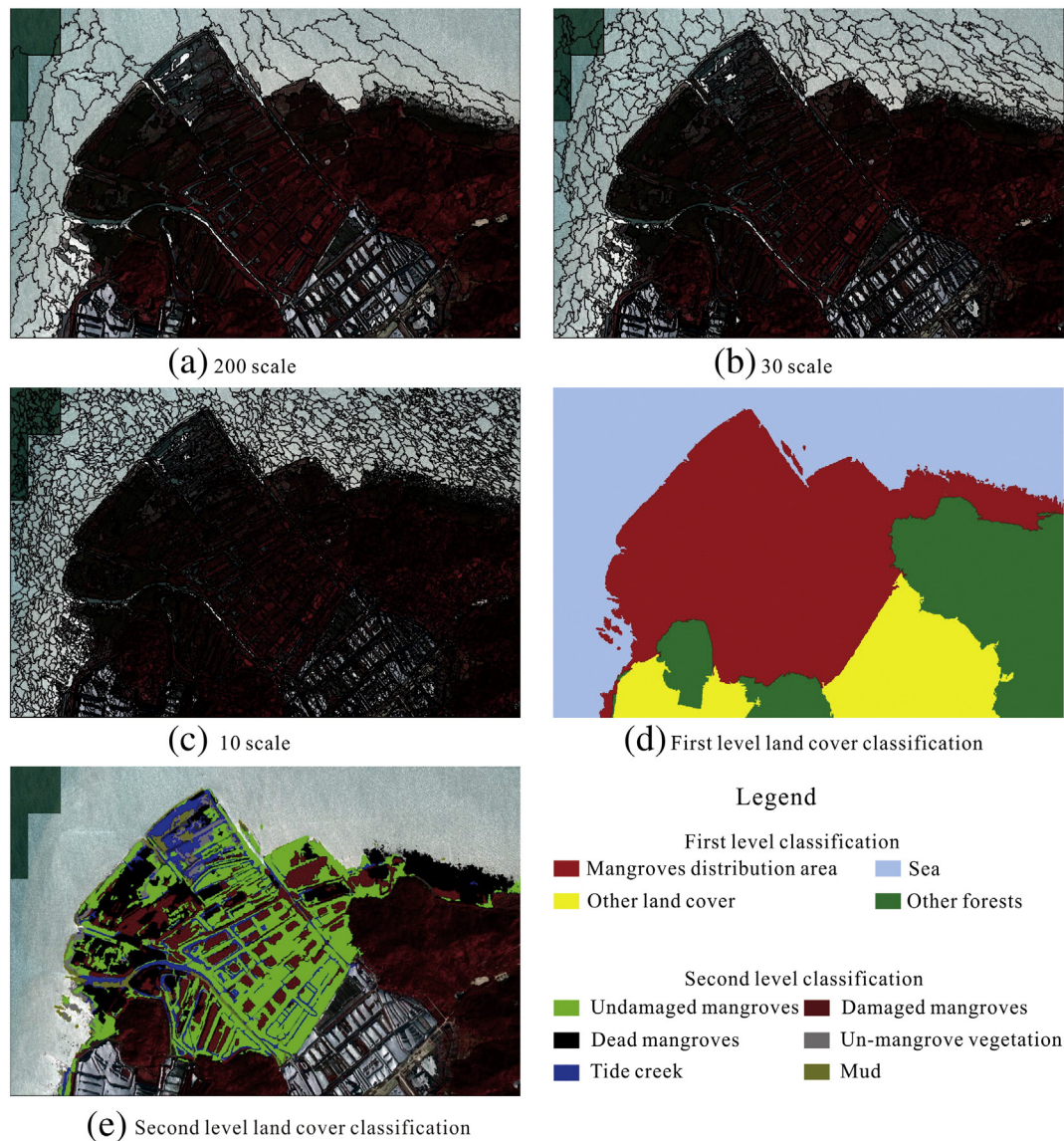


Fig. 6. Multi-scale segmentations and object-oriented classification results.

could also represent the possible effect of the age of mangroves, as most of the mangrove forests in Qi'ao Island are replanted and restored after 1999, from inland to the coastline. In addition, mangroves with different tree heights suffered different damages under the extreme cold weather. The tree height data of mangrove forests obtained from field survey and ASTER GDEM are used as the third variable for the effect of tree structure.

The freezing temperature of cold air can directly injure or kill the foliage of mangroves and the strong cold wind can break the branches or trunks of mangroves. The temperature and wind velocity during the blizzard at the regional scale determine the overall severity of cold damage to mangroves. The daily minimum temperature during the blizzard is 4.3 °C and wind velocity is 2.5 m/s. The coupled effect of wind direction and terrain topography influences the spatial variation of temperature and wind velocity at the local scale, which may cause the spatial difference in severity level of cold damage to mangroves. As shown by the wind rose diagram in Fig. 2, the prevailing wind direction during the blizzard is from the East. Fig. 8 shows the topography of Qi'ao Island. Hills are distributed along the northeast coast of the island, and the hill peaks have an elevation of about 100 m. The hills create windbreaks and shield land behind them from the wind (Fig. 7),

which protects the mangrove forest on the leeward side. This shielding effect decays with the increase of distance to the ridges of the hills. Using the ASTER GDEM, the surface slope and aspect were calculated and then the ridgeline of the hills was extracted. A series of buffer zones with 100 m interval was created in the leeward side of the hills to represent the distance to the ridgeline (Fig. 7b). The buffer zones within 500 m distance to the ridgeline are not considered since no mangrove trees are distributed within this range. It is expected that a shorter distance to the ridge line, the greater protection of hills to mangroves from the cold east wind.

3.2.2. Mangrove cold damage index (MCDI)

Both field observation and remote sensing images show spatial variation of the mangrove damage level. Those along the coast appear to be damaged most severely, while mangroves in the inland area are less damaged. The mangroves close to the hill ridges also appear less damaged by the blizzard. A mangrove cold damage index (MCDI) is created for quantitative analysis of climate and landscape effects through the two proxy distance variables. The index represents the cold damage intensity of mangroves in each distance buffer zone. A higher MCDI value indicates more severe damage to the mangroves.

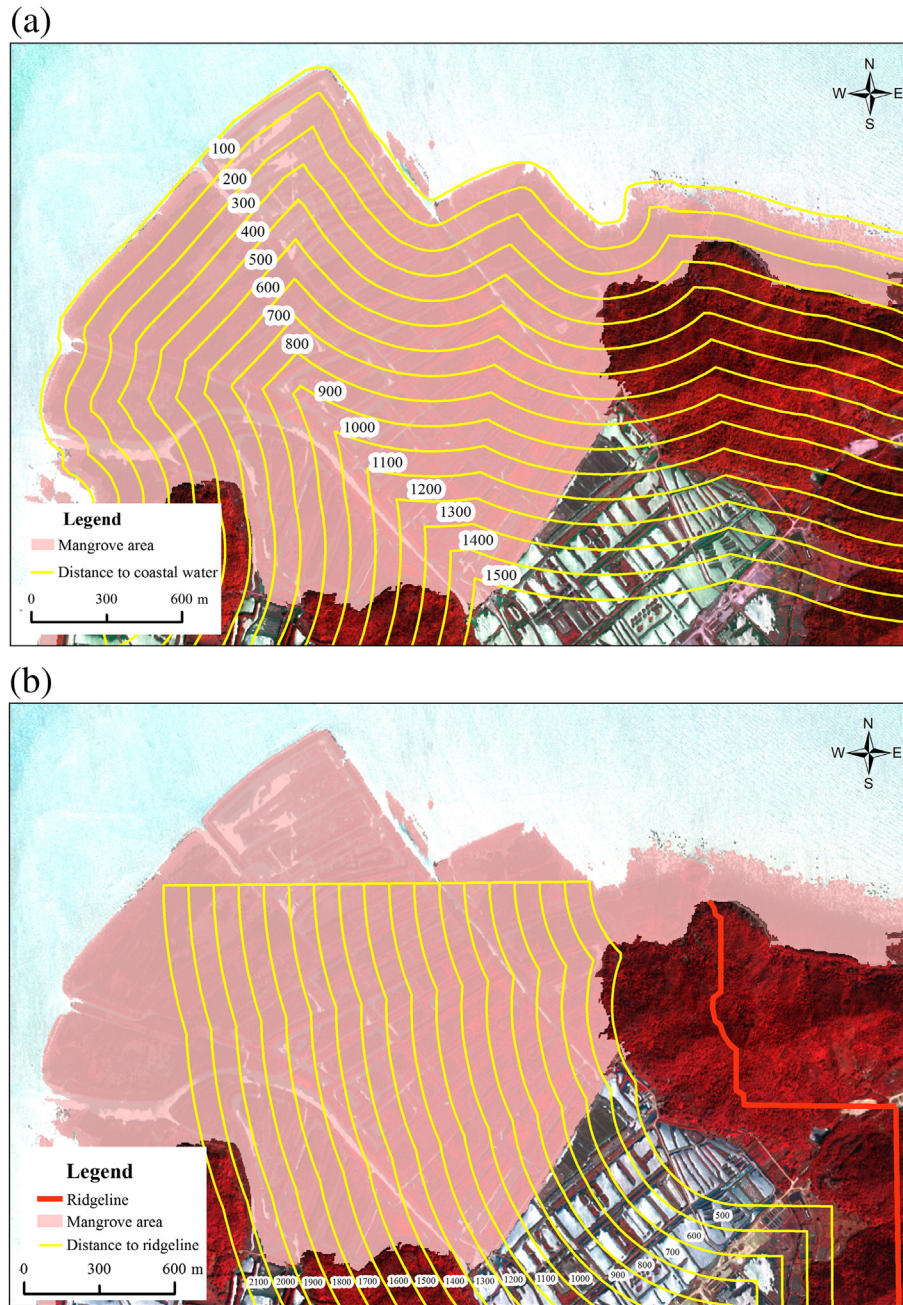


Fig. 7. Two proxy environmental variables for climate and landscape factors: a) distance to coastal water; b) distance to ridgeline of hills in the leeward side.

For each distance buffer zone, we calculate MCDI based on the remote sensing classification using the following equation:

$$MCDI = (1 * A_{d1} + 0.5 * A_{d2}) / (A_{d1} + A_{d2} + A_h) \quad (1)$$

where A_{d1} is the area ratio of dead mangroves in a distance buffer zone; and similarly, A_{d2} and A_h are the areal percentage of damaged and undamaged mangroves in a distance buffer zone, respectively. Obviously, the three percentages satisfy the following relation:

$$A_{d1} + A_{d2} + A_h = \text{Total area.} \quad (2)$$

3.2.3. Correspondence analysis

The correspondence analysis technique is employed to further examine the statistical association between severity level of cold

damage and the climate and landscape and biological factors, which include leeward side distance to the hill ridges, distance to the coastal water and tree height. The two distance variables are transformed into discrete category variables using the buffering operation. The leeward side distance to the hill ridges is transformed to a category variable with 17 discrete buffer zones from 500 m to 2100 m with an interval of 100 m. Similarly, the distance to the coastal water is converted into a category variable with 15 discrete buffer zones from 0 to 1500 m with an interval of 100 m. The tree height data of mangrove forests between 0 and 15 m is converted into a category variable with 15 zones with an interval of 1 m. The variable for the cold damage severity level of mangroves is represented by the three discrete categories from above classification: undamaged, damaged, and dead.

Correspondence analysis is a method of factoring categorical variables and displaying them in a property space, which maps their association in two or more dimensions. The multivariate nature of

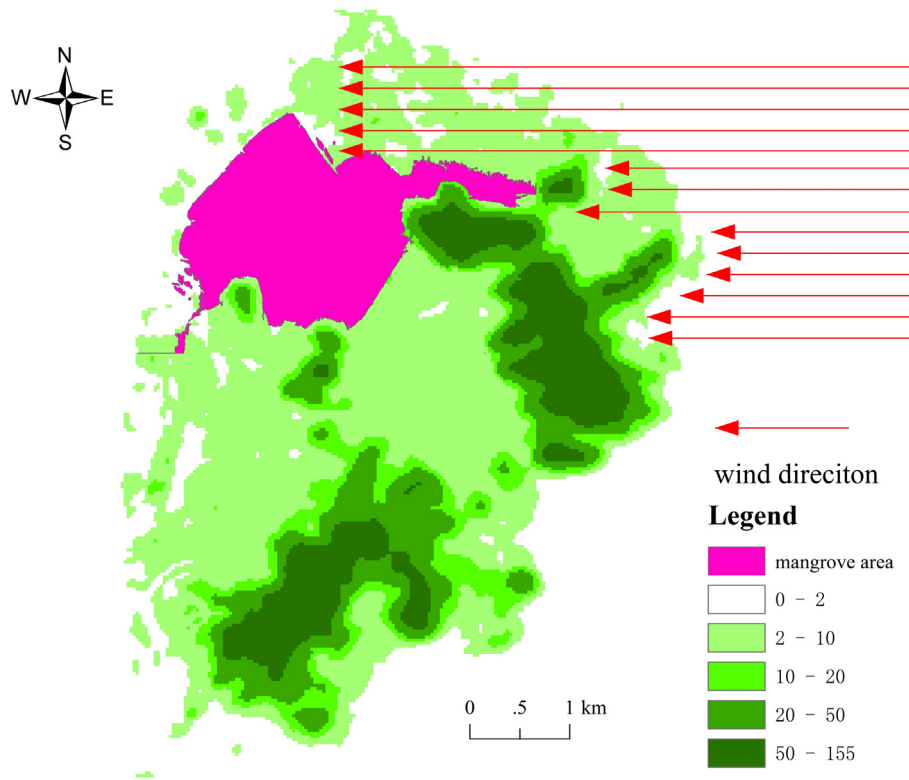


Fig. 8. Terrain and wind direction analysis of the Q'ao Island.

correspondence analysis can reveal relationships that would not be detected in a series of pair-wise comparisons of variables. Correspondence analysis analyzes two-way contingency tables containing some measure of correspondence between the categories of two discrete variables (rows and columns of the table). Correspondence analysis can uncover and describe systematic relations and associations between variables in large contingency tables when there are no (or a rather incomplete) a priori expectations as to the nature of those relations (Hill, 1974; Ross, Meeder, Sah, Ruiz, & Telesnicki, 2000; van der Heijden & de Leeuw, 1985). Correspondence analysis simultaneously considers multiple categorical variables. Its graphical display of row and column points in bi-plots can help reveal structural relationships among the variable categories and objects.

In this study, the correspondence analysis implemented in SPSS software is used to explore the association of the mangrove cold damage severity level variable with the leeward side distance to ridge, the distance to ocean water and the tree height. The correspondence analysis starts with the construction of contingency tables between two category variables. Using a stratified random sampling method, a total of 2000 samples are selected from different cold damage severity

categories of mangroves based on the area ratio of damaged mangroves and the total mangrove forests to construct the contingency tables.

4. Results

4.1. Classification results and accuracy assessment

An error contingency matrix (Table 2) depicts the land cover classification result versus the field-observed land cover type. The diagonal cells indicate a match between classification and observation. If the spectral signals are used as sole input variables, the classification accuracy is about 72%. Due to the defoliation and broken branches, dead mangrove forests cannot be well discriminated from bare muddy ground. The inclusion of NDVI as an additional input variable can effectively improve the classification accuracy, which clearly distinguishes dead mangroves from muddy ground. The overall accuracy is 90.96% and Kappa statistics is 0.89. It is also revealed that the shape and texture attributes are not helpful in improving classification accuracy. This is probably because all objects of cold damaged mangrove patch have similar size, area, and shape characteristics.

Table 2
Error matrix of object-oriented classification of cold damaged mangrove.

	TC	OV	DM	IM	HM	M	Total	User's accuracy
TC	24	0	0	0	0	1	25	96.0%
OV	0	20	0	0	0	1	21	95.2%
DM	0	1	21	3	0	0	25	84.0%
IM	0	0	3	29	5	0	37	78.4%
VM	0	1	0	1	39	0	41	95.1%
M	0	0	0	0	0	28	28	100%
Total	24	22	24	33	44	30	177	
Producer's accuracy	100%	90.9%	87.5%	87.9%	88.6%	93.3%		

Total accuracy = 90.96%; Kappa statistics = 0.89.

Note: DM = dead mangrove; IM = damaged mangrove; VM = undamaged mangrove; TC = tide creek; OV = other vegetation; M = mud.

Table 3

Accuracy comparison for classifications using different sets of attributes.

Attributes	Accuracy	Kappa statistics
Spectral	72.1%	0.676
Shape	57.7%	0.465
Texture	51.9%	0.391
NDVI	55.5%	0.411
Spectral + NDVI	80.7%	0.763
Spectral + shape	71.9%	0.673
Spectral + texture	69.6%	0.643
All attributes	83.5%	0.792

The user's accuracy, detailing errors of commission, ranges between 78.4% and 100%, and the producer's accuracy, detailing errors of omission, varies between 87.5% and 100%. Misclassification is mainly related to misidentifying the different types of cold damaged mangrove forests. The high overall classification accuracy indicates that high resolution multi-spectral IKONOS imagery contains sufficient spectral and spatial information for detecting the cold damage to mangroves and the object-oriented method with decision tree learning algorithms is suitable for classifying severity level of mangrove cold damage and different types of land covers.

The overall classification accuracy and Kappa values for different combination of input variables are summarized in Table 3.

As shown in Table 3, the spectral information is much more important for the mangrove damage classification than texture and shape information. The use of spectral attributes alone can achieve a classification accuracy of 72.1%. The addition of explicit vegetation attribute NDVI into spectral attributes results in a significant increase in classification accuracy by 8.6%. However, the inclusion of texture or shape attributes does not improve the classification accuracy. When all 24 attributes are blindly included, the classification accuracy is 83.5%, which is worse than the

classification accuracy (90.96%) achieved by using the five attributes selected by See5 winnowing function. This indicates that the selected attributes and the corresponding classification rule set from our decision tree learning method are efficient and effective for cold damaged mangrove classification.

The statistical analysis of this map shows that the area of undamaged mangrove forests, damaged mangrove forests, and dead mangrove forests is 140.61 ha, 71.97 ha, and 74.81 ha, respectively. Approximately 51.1% of mangrove forests in Qi'ao Island were either damaged or died as a result of the 2008 blizzard. This implies that remote sensing and geospatial technologies can provide the local management agency with valuable and timely information for the damage assessment and recovery of mangrove forests.

4.2. Spatial variation pattern of mangrove cold damage index

As shown in Fig. 9a, there is an overall pattern that the cold damage level (MCDI) decreases with the distance to coastal water. Namely, the mangroves closer to cold ocean water tend to be more seriously damaged. However, this pattern and tendency does not hold within 200 m coastal zone. Mangrove trees in the 200 meter buffer zone have suffered more serious cold damage than those in the 100 m buffer zone. According to field investigation, mangroves in the 200 meter buffer zone are newly planted, and these mangrove trees are little and more vulnerable to the cold compared with the established old mangrove trees in the 100 m buffer zone. In general, the mangroves planted close to coast are much shorter than the mangroves planted inland because taller mangroves cannot survive in the shore area due to the strong wind and tide. As shown in Fig. 9b, the hills protected in certain degree the mangroves in the leeward side within 1500 m of the ridgeline, and the MCDI is relatively small within this range. The wind shadow effect of the hills starts to fade rapidly beyond 1500 m from the ridgeline,

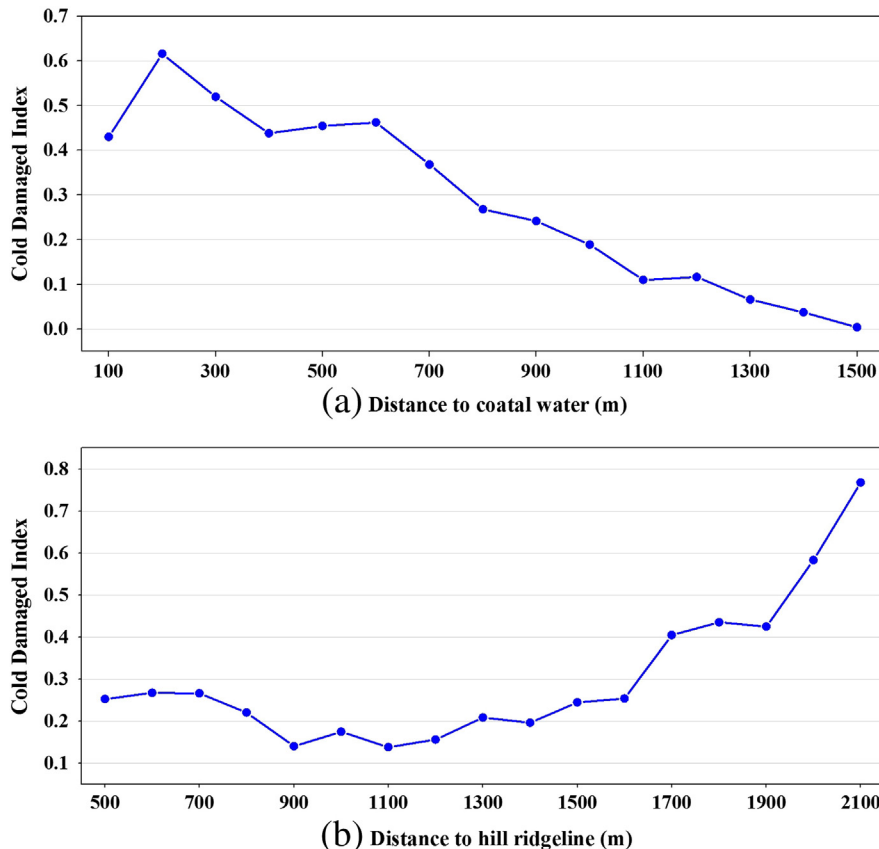


Fig. 9. Spatial pattern of MCDI: a) MCDI varies with distance to coastal water; b) MCDI varies with distance to hill ridgeline.

Table 4
Contingency table of distance buffer to hill ridgeline.

Distance buffer to hill ridgeline/m	Mangrove types		
	Undamaged	Damaged	Dead
500	26	4	5
600	49	12	5
700	39	22	8
800	64	16	6
900	59	15	0
1000	57	17	3
1100	69	20	1
1200	64	21	2
1300	45	25	4
1400	63	29	6
1500	53	11	9
1600	37	18	10
1700	26	43	17
1800	21	47	23
1900	36	28	12
2000	21	18	44
2100	7	24	36

Table 5
Contingency table of distance buffer to coastal water.

Distance buffer to coastal water/m	Mangrove types		
	Undamaged	Damaged	Dead
100	106	8	78
200	82	45	148
300	89	65	103
400	77	57	40
500	53	54	41
600	64	43	52
700	78	36	40
800	88	62	9
900	64	45	5
1000	59	46	3
1100	63	10	3
1200	44	18	0
1300	45	8	0
1400	23	2	0
1500	17	0	0

and the MCDI starts to increase with the distance to the hill ridges. From our field investigation, we observed that a large area of mangrove forests in the far northwest of the hill were dead or damaged. The area of these dead and damaged mangrove forests decreases from the 500 m buffer to the 900 m buffer, so does the MCDI. From the 900 m buffer to the 1500 m buffer, the MCDI increases slightly due to the gradual weakening of the wind shadow effect.

Table 6
Contingency table of tree height.

Tree height/m	Mangrove types		
	Undamaged	Damaged	Dead
0	33	39	54
1	28	43	55
2	54	59	13
3	46	61	18
4	59	55	11
5	58	63	5
6	93	30	3
7	75	44	6
8	100	25	0
9	73	45	8
10	75	48	3
11	75	50	0
12	51	46	29
13	38	45	43
14	40	26	59
15	20	23	83

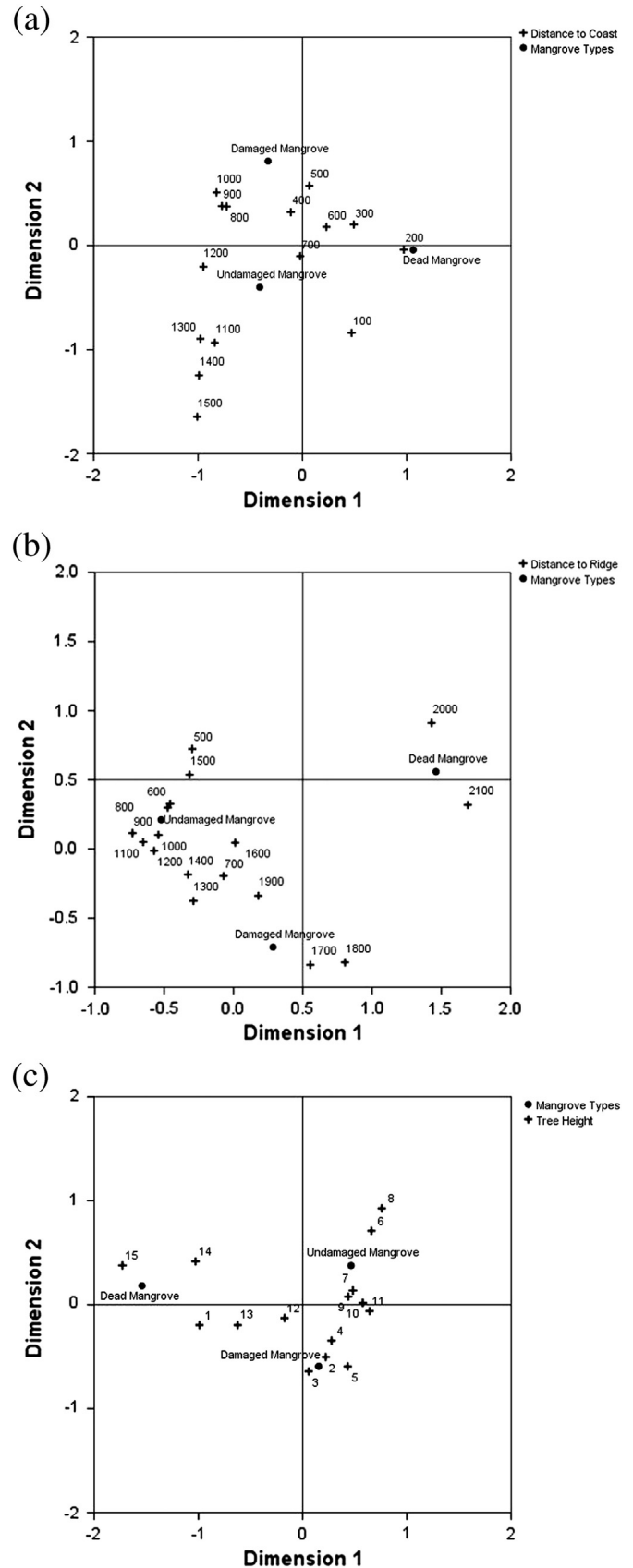


Fig. 10. Graphical displays of the results of the correspondence analysis of two spatial factors and types of cold damaged mangroves: a) distance to coastal water, b) distance to hill ridgeline, c) tree height.

4.3. Statistical association between severity levels of cold damage and influence factors

The resulting contingency tables between the category variable of cold damage severity level and the category variable of the distance to ocean, the leeward side distance to ridge and the tree height are shown in Tables 4, 5 and 6 respectively. From the two-way contingency tables, the correspondence analysis computes category profiles (relative frequency) and masses (marginal proportions), the Chi-square distances between these points, and the inertia (variance) of profile points that measures the extent to which profile points are spread around the centroid (the mean profile). Next, dimensionality reduction was conducted by first computing the variance/covariance matrix of variables and then selecting new axes/factors that explain maximum inertia (variance) of cloud points, as in principal component analysis. The final analysis results of correspondence analysis are presented graphically as bi-plots (Fig. 10), which show the configurations of points in projection planes, formed by the first two main axes/factors (Greenacre, 1992). The bi-plots visualize the associations between categories of two variables and facilitate interpretation. Categories with similar distributions are represented as points that are close in space (distinct clusters), and categories that have very dissimilar distributions will be positioned far apart as scattered points.

From Fig. 10a, it is clear that the undamaged mangroves are clustered in the inland (including 1100 m, 1200 m, 1300 m, 1400 m, and 1500 m buffer zones), damaged mangroves with mid-range distance buffer zones to ocean water (500 m, 600 m, 700 m, 800 m, 900 m, 1000 m buffer zones), and dead mangroves near the coastline (100 m, 200 m, and 300 m). This result suggests that the cold damage severity of mangrove forests is associated with proximity to ocean, possibly due to a combination of edge effect and age of mangroves.

Associations between mangrove cold damage severity and the leeward side distance to hill ridges are displayed in Fig. 10b. The undamaged mangroves that are not damaged by the blizzard tend to be clustered close to the hill ridges (500 m, ..., 1500 m), where are effectively protected from cold damage by the wind shadow effect of topographical hills. The damaged mangroves are clustered with intermediate distance buffer zones to the ridges (1600 m, 1700 m, 1800 m, 1900 m), which indicate that the wind shadow effect of hills is significantly reduced after cold air/wind crosses the hills by 1.5 km. The dead mangroves are clustered far away from the hill ridges (2000 m and 2100 m), which suggests that the wind shadow effect of the hills cannot reach the areas farther than 2 km from the hill ridges.

Tree height is closely associated with the cold damage (Fig. 10c). Dead mangroves are either the tallest (14–15 m) or the shortest (below 1 m). The tallest mangroves may be damaged by the strong cold wind, while the shortest by the cold temperature. This finding is consistent with that of Ross et al. (2009). They reported that variable tree height may influence cold damage and that patches of comparatively short trees may experience more damage, especially if surrounded by taller trees, which facilitates the pooling of cold air in nearby short trees. Damaged mangroves tend to be 2–5 m or 12–13 m in height, which can be explained by reasons similar to those of dead mangroves. Undamaged mangroves tend to have moderate height, ranging from 6 m to 11 m.

5. Discussion

This study has adopted an object-oriented method for discriminating different land cover types and mangrove forests of different cold damage levels from multi-spectral IKONOS imagery. The object-oriented classification is based on the use of spectral and vegetation attribute of image objects derived from multi-scale segmentations of IKONOS imagery. The case study in Qi'ao Island, South China demonstrates that the use of object-oriented method with decision tree learning algorithms on very high resolution IKONOS satellite images is effective in mapping spatial distribution of cold damage to mangrove forests.

Despite the overall high classification accuracy, the discrimination of damaged mangroves from undamaged and dead mangrove forests is still challenging with IKONOS multi-spectral imagery. As shown in Table 3, some damaged mangrove stands (image objects) were misclassified into undamaged or dead mangroves. The further improvement for the classification of mangroves of different cold damage levels may need satellite imagery that has higher spatial resolution and more spectral bands than IKONOS imagery, such as airborne hyperspectral imagery, and WorldView-2, which has 8 multi-spectral bands with a 2-m spatial resolution and a panchromatic band with a 0.5-m spatial resolution.

All dead mangroves were removed during the summer of 2008. The vegetation previously under the dead mangroves has grown rapidly. A WorldView-II image (Fig. 11a) captured on November 11 of 2010 shows the distribution of the understory, which mainly includes *A. ilicifolius*, *Spartina alterniflora* and *Acrostichum aureum* (Fig. 11b). The higher number of spectral bands in WorldView-II images allows for finer spectral classification than those of IKONOS images. The

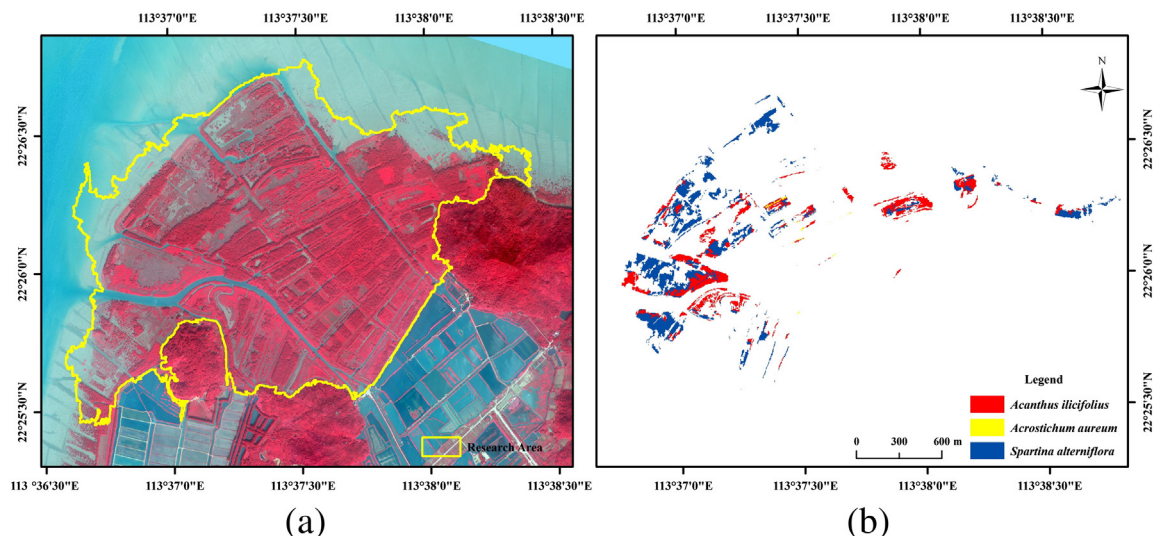


Fig. 11. WorldView-II image of the Mangrove Nature Reserve dated November 11, 2010, and the classification of the fast-growing understory after the removal of dead mangrove.

WorldView-II classification of the understory verifies the accuracy of the IKONOS classification of dead mangroves.

Overall many of the aforementioned findings are consistent with the literature (Ross et al., 2006, Ross et al., 2009). In addition, the study has discovered environmental and landscape factors that help mitigate cold damage to mangroves.

6. Conclusion

The ecological and societal values of mangrove forests, particularly their critical role as natural barriers and bioshields against hurricane and tsunami hazards, have been increasingly recognized. Many countries have launched various projects to restore and conserve mangrove wetlands to enhance the coastal resilience to natural hazards. However, the cold weather events often impose threat to the restoration and conservation efforts, particularly in subtropical and tropical coasts. This study represents the first research attempt to study the suitability of remote sensing technique for the assessment of mangrove cold damage.

Through a case study of mangroves in Qi'ao Island, located in tropical Southern China, the research has demonstrated that the high resolution multispectral satellite data such as IKONOS images contain sufficient information for detecting and mapping the damaged mangroves. The combined use of spectral, and NDVI variables with object-oriented classification method can achieve accurate discrimination of the mangroves with different severity levels of cold damage.

MCDI and correspondence analysis suggest that local terrain topography, wind direction and proximity to ocean water are important factors controlling the spatial distribution of mangrove cold damage. Tree height of mangroves is another important factor affecting mangrove forests under extreme cold weather. The leeward side of hills and mountains provides milder climate protecting mangroves from cold damage, and the mangroves near coast are more vulnerable due to the edge effects. To minimize possible cold damage and increase the survival rate, one can identify the leeward side of hills and mountains as potential rehabilitation sites for replanting mangroves or create artificial terrain in the upstream location of prevailing wind to protect downstream mangroves. One could also select and plant cold-resistance species and relatively large seedlings in the area nearby ocean to increase the root tolerance to cold water. In the events of the predicted cold weather, conservation and protection priorities should be given to mangroves located in the windward side and in the open flat coastal plain near ocean water. In sum, the study suggests that the knowledge and information about local climate and landscape controls can offer some useful insights on how to better conserve, protect and manage the mangrove forests in the future.

Acknowledgments

This study was supported by the National Science Foundation of China (Grant no. 41001291), the National Basic Research Program of China (973 Program) (Grant no. 2011CB707103), the Natural Science Foundation of Guangdong (Project no. 8151007003000008), and the Science and Technology Plan Project of Guangdong (Project no. 2010B030800003).

References

Alongi, D. (2008). Mangrove forests: Resilience, protection from tsunamis, and responses to global climate change. *Estuarine, Coastal and Shelf Science*, 76, 1–13.

Baatz, M., & Schape, A. (2000). Multiresolution segmentation: An optimization approach for high quality multi-scale image segmentation. *Journal of Photogrammetry and Remote Sensing*, 58, 12–23.

Baghdadi, N., & Oliveros, C. (2007). Potential of ASAR/Envisat data for mud bank monitoring in French Guiana compared to ASTER imagery. *Journal of Coastal Research*, 23, 1509–1517.

Barbier, E. (2006). Natural barriers to natural disasters: Replanting mangroves after the tsunami. *Frontiers in Ecology and the Environment*, 4, 124–131.

Benz, U. C., Hofmann, P., Willhauck, G., Lingenfelder, I., & Heynen, M. (2004). Multi-resolution, object-oriented fuzzy analysis of remote sensing data for GIS-ready information. *ISPRS Journal of Photogrammetry and Remote Sensing*, 58, 239–258.

Blasco, F., Gauquelin, T., Rasolofoharino, M., Denis, J., Aizpuru, M., & Caldiarou, V. (1998). Recent advances in mangrove studies using remote sensing data. *Marine and Freshwater Research*, 49, 287–296.

Blasco, F., Saenger, P., & Janodet, E. (1996). Mangroves as indicators of coastal change. *Catena*, 27, 167–178.

Chen, L., Wang, W., Zhang, Y., Huang, L., & Zhao, C. (2010). Damage to mangroves from extreme cold in early 2008 in southern China. *Chinese Journal of Plant Ecology*, 34, 186–194.

Conchedda, G., Durieux, L., & Mayaux, P. (2008). An object-based method for mapping and change analysis in mangrove ecosystems. *ISPRS Journal of Photogrammetry and Remote Sensing*, 63, 578–589.

Congalton, R. G. (1988). A comparison of sampling schemes used in generating error matrices for assessing the accuracy of maps generated from remotely sensed data. *Photogrammetric Engineering & Remote Sensing*, 54, 593–600.

Congalton, R. G., & Mead, R. A. (1986). Review of three discrete multivariate analysis techniques used in assessing the accuracy of remotely sensed data from error matrices. *IEEE Transactions on Geoscience and Remote Sensing*, GE-24, 169–174.

Dahdouh-Guebas, F., Jayatissa, L., Di Nitto, D., Bosire, J., Lo Seen, D., & Koedam, N. (2005). How effective were mangroves as a defence against the recent tsunami? *Current Biology*, 15, R443–R447.

Dahdouh-Guebas, F., Van Pottelbergh, I., Kairo, J. G., Cannicci, S., & Koedam, N. (2004). Human-impacted mangroves in Gazi (Kenya): Predicting future vegetation based on retrospective remote sensing, social surveys, and tree distribution. *Marine Ecology Progress Series*, 272, 77–92.

Danielsen, F., Sorensen, M., Olwig, M., Selvam, V., Parish, F., Burgess, N., et al. (2005). The Asian tsunami: A protective role for coastal vegetation. *Science (Washington)*, 310, 643.

DeFries, R. S., & Chan, J. C. W. (2000). Multiple criteria for evaluating machine learning algorithms for land cover classification from satellite data. *Remote Sensing of Environment*, 74, 503–515.

Dronova, I., Gong, P., & Wang, L. (2011). Object-based analysis and change detection of major wetland cover types and their classification uncertainty during the low water period at Poyang Lake, China. *Remote Sensing of Environment*, 115, 3220–3236.

Duro, D. C., Franklin, S. E., & Dubé, M. G. (2012). A comparison of pixel-based and object-based image analysis with selected machine learning algorithms for the classification of agricultural landscapes using SPOT-5 HRG imagery. *Remote Sensing of Environment*, 118, 259–272.

Ellison, A.M., & Farnsworth, E. J. (1996). Anthropogenic disturbance of Caribbean mangrove ecosystems: Past impacts, present trends, and future predictions. *Biotropica*, 549–565.

Everitt, J. H., & Judd, F. W. (1989). Using remote sensing techniques to distinguish and monitor black mangrove (*Avicennia germinans*). *Journal of Coastal Research*, 5, 737–745.

Everitt, J. H., Yang, C., Sriharan, S., & Judd, F. W. (2008). Using high resolution satellite imagery to map black mangrove on the Texas Gulf Coast. *Journal of Coastal Research*, 24, 1582–1586.

Franklin, J. (1993). Discrimination of tropical vegetation types using SPOT multispectral data. *Geocarto International*, 8, 57–63.

Fromard, F., Vega, C., & Proisy, C. (2004). Half a century of dynamic coastal change affecting mangrove shorelines of French Guiana. A case study based on remote sensing data analyses and field surveys. *Marine Geology*, 208, 265–280.

Gao, J. (1998). A hybrid method toward accurate mapping of mangroves in a marginal habitat from SPOT multispectral data. *International Journal of Remote Sensing*, 19, 1887–1899.

Giri, C., Zhu, Z., Tieszen, L., Singh, A., Gillette, S., & Kelmelis, J. (2008). Mangrove forest distributions and dynamics (1975–2005) of the tsunami-affected region of Asia. *Journal of Biogeography*, 35, 519–528.

Green, E. P., Clark, C. D., Mumby, P. J., Edwards, A. I., & Ellis, A.C. (1998). Remote sensing techniques for mangrove mapping. *International Journal of Remote Sensing*, 19, 935–956.

Greenacre, M. (1992). Correspondence analysis in medical research. *Statistical Methods in Medical Research*, 1, 97–117.

Hansen, M., Dubayah, R., & Defries, R. (1996). Classification trees: An alternative to traditional land cover classifiers. *International Journal of Remote Sensing*, 17, 1075–1081.

Harakunarak, A., & Aksornkoae, S. (2005). Life-saving belts: Post-tsunami reassessment of mangrove ecosystem values and management in Thailand. *Tropical Coasts*, 48–55.

Hayakawa, Y., Oguchi, T., & Lin, Z. (2008). Comparison of new and existing global digital elevation models: ASTER G-DEM and SRTM-3. *Geophysical Research Letters*, 35, L17404.

Held, A., Ticehurst, C., Lymburner, L., & Williams, N. (2003). High resolution mapping of tropical mangrove ecosystems using hyperspectral and radar remote sensing. *International Journal of Remote Sensing*, 24, 2739–2759.

Heumann, B. W. (2011). Satellite remote sensing of mangrove forests: Recent advances and future opportunities. *Progress in Physical Geography*, 35, 87.

Hill, M.O. (1974). Correspondence analysis: A neglected multivariate method. *Journal of Applied Statistics*, 23, 340–354.

Jiang, L., & Huang, R. (2008). Investigation of the chilling damaged on mangrove and study on the cold tolerance of *Sonneratia apetala*. *Journal of Meteorological Research and Application*, 29 (35–28).

Kathiresan, K., & Rajendran, N. (2005). Coastal mangrove forests mitigated tsunami. *Estuarine, Coastal and Shelf Science*, 65, 601–606.

Kovacs, J. M., Flores-Verdugo, F., Wang, J., & Aspden, L. P. (2004). Estimating leaf area index of a degraded mangrove forest using high spatial resolution satellite data. *Aquatic Botany*, 80, 13–22.

- Kovacs, J. M., Vandenberg, C. V., Wang, J., & Flores-Verdugo, F. (2008). The use of multipolarized spaceborne SAR backscatter for monitoring the health of a degraded mangrove forest. *Journal of Coastal Research*, 24, 248–254.
- Kovacs, J. M., Wang, J., & Blanco-Correa, M. (2001). Mapping disturbances in a mangrove forest using multi-date Landsat TM imagery. *Environmental Management*, 27, 763–776.
- Kuenzer, C., Bluemel, A., Gebhardt, S., Quoc, T. V., & Dech, S. (2011). Remote sensing of mangrove ecosystems: A review. *Remote Sensing*, 3, 878–928.
- Laba, M., Blair, B., Downs, R., Monger, B., Philpot, W., Smith, S., et al. (2010). Use of textural measurements to map invasive wetland plants in the Hudson River National Estuarine Research Reserve with IKONOS satellite imagery. *Remote Sensing of Environment*, 114, 876–886.
- Laliberte, A. S., Fredrickson, E. L., & Rango, A. (2007). Combining decision trees with hierarchical object-oriented image analysis for mapping arid rangelands. *Photogrammetric Engineering and Remote Sensing*, 73, 197–207.
- Laliberte, A. S., Rango, A., Havstad, K. M., Paris, J. F., Beck, R. F., McNeely, R., et al. (2004). Object-oriented image analysis for mapping shrub encroachment from 1937 to 2003 in southern New Mexico. *Remote Sensing of Environment*, 93, 198–210.
- Li, M., Liao, B., Guan, W., Zheng, S., & Chen, Y. (2009). Survey on cold damage of mangroves in Guangdong Province. *Protection Forest Science and Technology*, 29–31.
- Li, Y., Zheng, D., Chen, H., Liao, B., Zheng, S., & Chen, X. (1998). Preliminary study on introduction of mangrove *Sonneratia apetala* Buch Ham. *Forest Research*, 39–44.
- Liu, K., Li, X., Shi, X., & Wang, S. (2008). Monitoring mangrove forest changes using remote sensing and GIS data with decision-tree learning. *Wetlands*, 28, 336–346.
- Long, B. G., & Skewes, T. D. (1996). A technique for mapping mangroves with Landsat TM satellite data and geographic information system. *Estuarine, Coastal and Shelf Science*, 43, 373–381.
- Mathieu, R., Aryal, J., & Chong, A. K. (2007). Object-based classification of IKONOS imagery for mapping large-scale vegetation communities in urban areas. *Sensors*, 7, 2860–2880.
- Mitri, G. H., & Gitas, I. Z. (2004). A performance evaluation of a burned area object-based classification model when applied to topographically and non-topographically corrected TM imagery. *International Journal of Remote Sensing*, 25, 2863–2870.
- Murray, M. R., Zisman, S. A., Furley, P. A., Munro, D.M., Gibson, J., Ratter, J., et al. (2003). The mangroves of Belize part 1. Distribution, composition and classification. *Forest Ecology and Management*, 174, 265–279.
- Nishii, R., & Tanaka, S. (1999). Accuracy and inaccuracy assessments in land-cover classification. *IEEE Transactions on Geoscience and Remote Sensing*, 37, 491–498.
- Pasqualini, V., Iltis, J., Dessay, N., Lointier, M., Guelorget, O., & Polidori, L. (1999). Mangrove mapping in North-Western Madagascar using SPOT-XS and SIR-C radar data. *Hydrobiologia*, 413, 127–133.
- Quinlan, J. R. (1990). Decision trees and decision-making. *IEEE Transactions on Systems, Man, and Cybernetics*, 20, 339–346.
- Quinlan, J. R. (1996). Learning decision tree classifiers. *ACM Computing Surveys*, 28, 71–72.
- Quinlan, J. R. (1999). Simplifying decision trees. *International Journal of Human Computer Studies*, 51, 497–510.
- Raši, R., Bodart, C., Stibig, H. -J., Eva, H., Beuchle, R., Carboni, S., et al. (2011). An automated approach for segmenting and classifying a large sample of multi-date Landsat imagery for pan-tropical forest monitoring. *Remote Sensing of Environment*, 115, 3659–3669.
- Ren, H., Jian, S., Lu, H., Zhang, Q., Shen, W., Han, W., et al. (2008). Restoration of mangrove plantations and colonisation by native species in Leizhou Bay, South China. *Ecological Research*, 23, 401–407.
- Ren, H., Wu, X., Ning, T., Huang, G., Wang, J., Jian, S., et al. (2011). Wetland changes and mangrove restoration planning in Shenzhen Bay, Southern China. *Landscape and Ecological Engineering*, 7, 241–250.
- Ross, M., Meeder, J., Sah, J., Ruiz, P., & Telesnicki, G. (2000). The southeast saline Everglades revisited: 50 years of coastal vegetation change. *Journal of Vegetation Science*, 11, 101–112.
- Ross, M. S., Ruiz, P. L., Sah, J. A. Y. P., & Hanan, E. J. (2009). Chilling damage in a changing climate in coastal landscapes of the subtropical zone: A case study from south Florida. *Global Change Biology*, 15, 1817–1832.
- Ross, M. S., Ruiz, P. L., Sah, J. P., Reed, D. L., Walters, J., & Meeder, J. F. (2006). Early post-hurricane stand development in fringe mangrove forests of contrasting productivity. *Plant Ecology*, 185, 283–297.
- Sanford, M. P. (2009). Valuating mangrove ecosystems as coastal protection in post-tsunami South Asia. *Natural Areas Journal*, 29, 91–95.
- Scepan, M. H. J. (June 2002). Object-oriented mapping and analysis of urban land use/cover using IKONOS data. *Proceedings of 22nd EARSEL symposium "Geoinformation for European-wide integration"* (Prague).
- Sheridan, P., & Hays, C. (2003). Are mangroves nursery habitat for transient fishes and decapods? *Wetlands*, 23, 449–458.
- Stevens, P. W., Fox, S. L., & Montague, C. L. (2006). The interplay between mangroves and saltmarshes at the transition between temperate and subtropical climate in Florida. *Wetlands Ecology and Management*, 14, 435–444.
- Stuart, S., Choat, B., Martin, K., Holbrook, N., & Ball, M. (2007). The role of freezing in setting the latitudinal limits of mangrove forests. *New Phytologist*, 173, 576–583.
- Sulong, I., Mohd-Lokman, H., Mohd-Tarmizi, K., & Ismail, A. (2002). Mangrove mapping using Landsat imagery and aerial photographs: Kemaman District, Terengganu, Malaysia. *Environment, Development and Sustainability*, 4, 135–152.
- Tanaka, N., Sasaki, Y., Mowjood, M., Jinadasa, K., & Homchuen, S. (2007). Coastal vegetation structures and their functions in tsunami protection: Experience of the recent Indian Ocean tsunami. *Landscape and Ecological Engineering*, 3, 33–45.
- Thu, P.M., & Populus, J. (2007). Status and changes of mangrove forest in Mekong Delta: Case study in Tra Vinh, Vietnam. *Estuarine, Coastal and Shelf Science*, 71, 98–109.
- Vaiphasa, C., Skidmore, A. K., & de Boer, W. F. (2006). A post-classifier for mangrove mapping using ecological data. *ISPRS Journal of Photogrammetry and Remote Sensing*, 61, 1–10.
- Valiela, I., Bowen, J., & York, J. (2001). Mangrove forests: One of the world's threatened major tropical environments. *Bioscience*, 51, 807–815.
- van der Heijden, P. G. M., & de Leeuw, J. (1985). Correspondence analysis used complementary to loglinear analysis. *Psychometrika*, 50, 429–447.
- Vijay, V., Biradar, R. S., Inamdar, A.B., Deshmukhe, G., Baji, S., & Pikle, M. (2005). Mangrove mapping and change detection around Mumbai (Bombay) using remotely sensed data. *Indian Journal of Marine Sciences*, 34, 310–315.
- Walker, J. S., & Briggs, J. M. (2007). An object-oriented approach to urban forest mapping in Phoenix. *Photogrammetric Engineering and Remote Sensing*, 73, 577–583.
- Wang, Y., Bonyne, G., Nugranad, J., Traber, M., Ngusaru, A., Tobey, J., et al. (2003). Remote sensing of mangrove change along the Tanzania coast. *Marine Geodesy*, 26, 35–48.
- Wang, L., Sousa, W. P., Gong, P., & Biging, G. S. (2004). Comparison of IKONOS and QuickBird images for mapping mangrove species on the Caribbean coast of Panama. *Remote Sensing of Environment*, 91, 432–440.
- Xiao, Z., Chen, Y., & Xie, S. (2004). Investigation on freeze injury of *Sonneratia caseolaris* (L.) Engl. and *S. apetala* Buch-Ham in Shantou. *Protection Forest Science and Technology*, 24–31.
- Yu, Q., Gong, P., Clinton, N., Biging, G., Kelly, M., & Schirokauer, D. (2006). Object-based detailed vegetation classification with airborne high spatial resolution remote sensing imagery. *Photogrammetric Engineering and Remote Sensing*, 72, 799–811.
- Zhang, K., Simard, M., Ross, M., Rivera-Monroy, V. H., Houle, P., Ruiz, P., et al. (2008). Airborne laser scanning quantification of disturbances from hurricanes and lightning strikes to mangrove forests in Everglades National Park, USA. *Sensors*, 8, 2262–2292.